Biochemistry and Biophysics Reports 39 (2024) 101790

Contents lists available at ScienceDirect

Biochemistry and Biophysics Reports

journal homepage: www.elsevier.com/locate/bbrep

Generation of bone-specific lysyl hydroxylase 2 knockout mice and their phenotypes

Kenta Tsuneizumi [a], Atsushi Kasamatsu [b,**], Tomoaki Saito [a], Reo Fukushima [c], Yuki Taga [d], Kazunori Mizuno [d], Masataka Sunohara [e], Katsuhiro Uzawa [a,b,*], Mitsuo Yamauchi [c,***]

[a] Department of Oral Science, Graduate School of Medicine, Chiba University, Chiba, Japan
[b] Department of Dentistry and Oral-Maxillofacial Surgery, Chiba University Hospital, Chiba, Japan
[c] Division of Oral and Craniofacial Health Sciences, Adams School of Dentistry, University of North Carolina at Chapel Hill, Chapel Hill, NC, United States
[d] Nippi Research Institute of Biomatrix, Ibaraki, Japan
[e] Department of Anatomy, School of Life Dentistry at Tokyo, Nippon Dental University, Tokyo, Japan

ARTICLE INFO

Keywords:
Lysyl hydroxylase 2
Collagen cross-link
Bone-specific conditional knockout

ABSTRACT

Lysyl hydroxylase 2 (LH2) catalyzes the hydroxylation of lysine residues in the telopeptides of type I collagen. This modification is critical for the formation of stable hydroxylysine-aldehyde derived collagen cross-links, thus, for the stability of collagen fibrils. Though dysfunction of LH2 causes Bruck syndrome, recessive osteogenesis imperfecta with joint contracture, the molecular mechanisms by which LH2 affects bone formation are still not well understood. Since the *Plod2* knockout mice are embryonically lethal, we generated bone-specific LH2 conditional knockout mice (bsLH2-cKO) using the osteocalcin-Cre/loxP system, and evaluated phenotypes of femurs. LH2 mRNA and protein levels assessed by qPCR, immunohistochemistry and Data Independent Acquisition proteomics were all markedly low in bsLH2-cKO femurs when compared to controls. Lysine hydroxylation of both carboxy- and amino-terminal telopeptides of an α1(I) chain were significantly diminished resulting in reduction of the hydroxylysine-aldehyde derived cross-links. The collagen fibrils in bsLH2-cKO appeared to be thicker, often fused and irregular when compared to controls. In addition, bone mineral density and mechanical properties of bsLH2-cKO femurs were significantly impaired. Taken together, these data demonstrate that LH2-catalyzed modification and consequent cross-linking of collagen are critical for proper bone formation and mechanical strength.

1. Introduction

Collagens represent a large family of structurally related proteins involving more than 40 distinct genes that produce at least 28 distinct collagen types [1]. Among these members, fibril-forming type I collagen (Col1) is the most abundant type in vertebrates providing tissues with form and stability. It is a heterotrimeric molecule composed of two α1 and one α2 chain, and the molecule consists of three structural domains: an amino (N)-terminal non-helical (N-telopeptide), a central triple helical and a carboxy (C)-terminal non-helical domains (C-telopeptide) [2]. They are packed into a fibril in the extracellular space. The biosynthesis of Col1 involves a number of post-translational modifications (PTMs) in- and outside of the cell. One of the unique and functionally critical PTMs are those of specific lysine (Lys) residues, i.e. 5-hydroxylation, mono- and di-glycosylation of hydroxylysine (Hyl) residues that occur in the endoplasmic reticulum (ER), then oxidative deamination of Lys and Hyl in both N- and C-telopeptides and finally the formation of covalent cross-links in the extracellular space [2]. These Lys PTMs, except the final cross-linking reactions, are catalyzed by specific enzyme groups such as lysyl hydroxylases 1–3 (LH1-3) for Lys hydroxylation, glycosyltransferase 25 domain containing (GLT25D) 1 and 2 for galactosylation of Hyl forming galactosylhydroxylysine (G-Hyl), LH3 for glucosylation of G-Hyl forming glucosylgalactosylhydroxylysine (GG-Hyl) and lysyl oxidases (LOXs) for oxidative deamination of telopeptisyl Lys and Hyl forming reactive Lys aldehyde (Lys^{ald}) and Hyl^{ald}, respectively. The aldehydes then spontaneously undergo a

* Corresponding author. Department of Oral Science, Graduate School of Medicine, Chiba University, Chiba, Japan.
** Corresponding author.
*** Corresponding author.
E-mail addresses: kasamatsua@faculty.chiba-u.jp (A. Kasamatsu), uzawak@faculty.chiba-u.jp (K. Uzawa), Mitsuo_Yamauchi@unc.edu (M. Yamauchi).

https://doi.org/10.1016/j.bbrep.2024.101790
Received 3 March 2024; Received in revised form 2 July 2024; Accepted 16 July 2024
Available online 19 July 2024

series of condensation reactions to form covalent intra- and intermolecular cross-links. The extent of these Lys modifications varies from tissue to tissue and provides the basis for the tissue-specific cross-linking pattern, i.e. quantity, types and maturation [2]. The abnormal Lys modifications and cross-linking directly cause and/or associated with various pathologies such as Ehlers-Danlos syndrome type VI [3,4], hyperelastosis cutis [5], osteoporosis [6], fibrosis/keloid [7–10], recessive dystrophic epidermolysis bullosa [11,12], recessive osteogenesis imperfecta [13–16].

Among LH family members, LH2 is unique in its ability to hydroxylate Lys and Hyl residues in telopeptides [7,17–19] and this function apparently cannot be compensated by other LH family members [20]. Since the telopeptidyl Hyl^{ald}-derived cross-links are chemically stable, LH2 is a critical determinant for the stability of collagen fibrils [20]. Dysfunction of both LH2 and its chaperone molecule FKBP65 [21,22] results in the lack of Lys hydroxylation in Col1 telopeptides that causes a rare autosomal recessive osteogenesis imperfecta, Bruck syndrome (BS) types II and I, respectively. Both types are clinically indistinguishable [23] indicating the cause of both BR types to be the defective LH2 activity.

Though these studies demonstrate the critical role of LH2 in BS, it is still not clear if the bone phenotype is a result of net effect of global LH2 disfunction or specific to bone without been affected by other tissues and organs. We previously reported that the global LH2 knockout (KO) mice die at an early embryonic stage [24]. Thus, to obtain insight into the function of LH2 in bone formation *in vivo*, we generated bone-specific LH2 conditional knockout mice (bsLH2-cKO) mice using the osteocalcin (OC)-Cre/loxP system and investigated the effects of bsLH2-cKO on bone at biochemical, morphological and biomechanical levels.

2. Materials and methods

2.1. Ethics statement

Animals were cared for following the guidelines of Chiba University. All of the animal experiments were approved by the Chiba University Review Board for Animal Care (Protocol, A29-212). The present study was reported in accordance with the ARRIVE 2.0 Essential 10 guidelines (https://arriveguidelines.org). All mice were housed under diurnal lighting conditions and allowed free access to food and water.

2.2. Generation of LH2$^{F/F}$ OC-Cre mice

LH2F$^{/F}$ OC-Cre (bsLH2-cKO) mice were generated according to the protocol in Supplemental Materials and Methods.

2.3. Polymerase chain reaction (PCR)

Genotyping and Cre-mediated DNA recombination were analyzed by PCR using specific primer sets. The PCR primers list has been described previously [25]. Briefly, PCR was carried out in a 50 μl reaction volume containing 0.25 μl Ex Taq polymerase (TaKaRa, Shiga, Japan), 4 μl dNTP mix (TaKaRa), 1 μl of each primer, 5 μl Ex Taq buffer (TaKaRa), 5 μl cDNA, and 33.75 μl nuclease-free water. The reaction was performed at 94 °C for 2 min, followed by 33 cycles of 94 °C for 30 s, 60 °C for 35 s, 72 °C for 35 s, and a final extension cycle at 72 °C for 5 min. The PCR product size was determined by electrophoresis on 3 % agarose gels.

2.4. Histological and immunohistochemical analyses

4-μm sections of paraffin-embedded femurs were cut and subjected to hematoxylin and eosin (H&E), Picrosirius Red (PSR), and immunohistochemical (IHC) analyses, according to the protocol in Supplemental Materials and Methods.

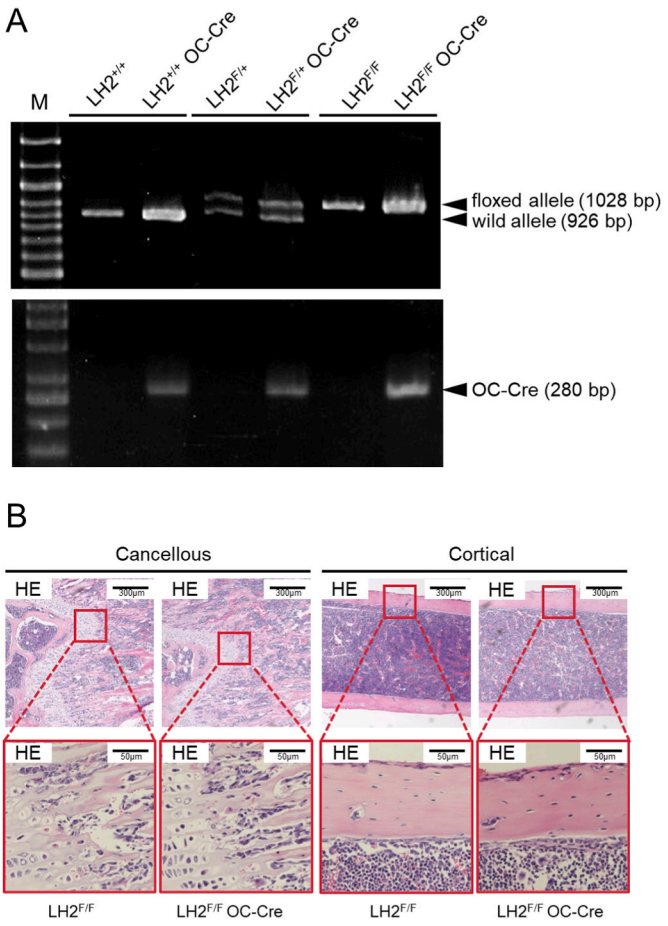

Fig. 1. Establishment of LH2$^{F/F}$ OC-Cre mice and evaluation of LH2 levels by immunohistochemical analyses. (A) Confirmation of bsLH2-cKO in tails by genotyping PCR. Genomic DNA was extracted from the tails of six types of mice (LH2$^{+/+}$, LH2$^{+/+}$ OC-Cre, LH2$^{F/+}$, LH2$^{F/+}$ OC-Cre, LH2$^{F/F}$, and LH2$^{F/F}$ OC-Cre). Floxed allele, 1028 bp; wild allele, 926 bp. **(B)** Representative HE images of femurs from LH2$^{F/F}$ and LH2$^{F/F}$ OC-Cre mice. There are no evident differences in cancellous and cortical regions of femurs between the LH2$^{F/F}$ and LH2$^{F/F}$ OC-Cre mice. Original magnification, ×40 and × 200; Scale bars, 300 μm and 50 μm.

2.5. Data Independent Acquisition (DIA) proteomic analysis

DIA proteomic analysis was performed to characterize and evaluate protein levels in the femurs of LH2$^{F/F}$ and LH2$^{F/F}$ OC-Cre mice (n = 3), according to the protocol described previously [26]. Volcano plots were evaluated for protein expression variation between the LH2$^{F/F}$ and LH2$^{F/F}$ OC-Cre mice.

2.6. Characterization of collagen fibrils and bone properties

In this study, we used femurs obtained from 8-week-old male mice. To assess the morphology of femurs, transmission electron microscope (TEM), micro-computed tomography (μCT) analysis, and three-point bending test were performed according to the protocol in Supplemental Materials and Methods.

2.7. Cross-link and Lys modifications of telopeptides in Col1

Collagen cross-links and site occupancy of Lys hydroxylation in the telopeptides of Col1 were analyzed according to the protocol in Supplemental Materials and Methods.

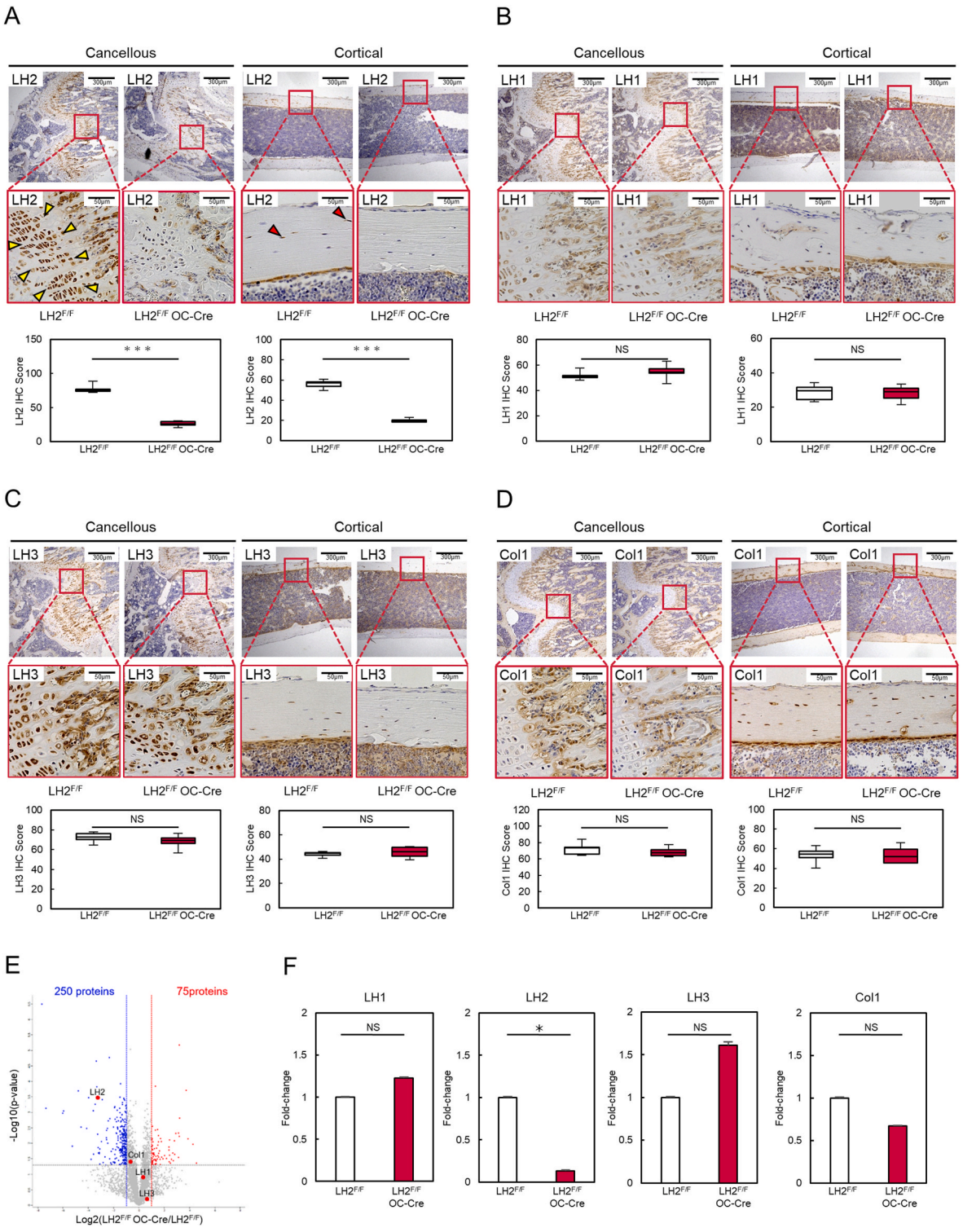

(caption on next page)

Fig. 2. Evaluation of LH1, LH2, LH3 and Col1 levels by IHC and Proteomic analysis of femurs in LH2$^{F/F}$ OC-Cre mice. Representative IHC images for LH1, LH2, LH3 and Col1 in cancellous and cortical regions of femurs from LH2$^{F/F}$ and LH2$^{F/F}$ OC-Cre mice. LH1, LH2, LH3 and Col1 expression levels are not significantly different between LH2$^{F/F}$ and LH2$^{F/F}$ OC-Cre femurs. Original magnification, ×40 and × 200; Scale bars, 300 μm and 50 μm. DIA proteomics in LH2$^{F/F}$ and LH2$^{F/F}$ OC-Cre femurs (n = 3). **(A)** Representative IHC images for LH2 in cancellous and cortical regions of femurs from LH2$^{F/F}$ and LH2$^{F/F}$ OC-Cre mice. In LH2$^{F/F+}$ femurs, intense immunoreactivities are evident in the areas of cancellous and cortical bone when compared to those from LH2$^{F/F}$ OC-Cre mice. Original magnification, ×40 and × 200; Scale bars, 300 μm and 50 μm. LH2 levels were calculated by the IHC scoring system (n = 3). The LH2 IHC scores for the cells of the cancellous bone ranged from 72.3 to 88.8 (median, 76.2) and 20.6 to 30.6 (median, 25.6) in LH2$^{F/F}$ and LH2$^{F/F}$ OC-Cre mice, respectively. The LH2 IHC scores for the cells of the cortical bone ranged from 49.8 to 60.9 (median, 57.3) and 18.0 to 23.2 (median, 20.0) in LH2$^{F/F}$ and LH2$^{F/F}$ OC-Cre mice, respectively. LH2 levels in LH2$^{F/F}$ OC-Cre femurs are significantly lower than those of LH2$^{F/F}$ femurs. ***$P < 0.001$. **(B)** LH1 levels are calculated by the IHC scoring system (n = 3). The LH1 IHC scores for the cells of the cancellous bone ranged from 47.9 to 57.7 (median, 50.4) and 45.4 to 62.8 (median, 54.3) in LH2$^{F/F}$ and LH2$^{F/F}$ OC-Cre mice, respectively. The LH1 IHC scores for the cells of the cortical bone ranged from 23.0 to 34.4 (median, 29.5) and 21.5 to 33.5 (median, 28.9) in LH2$^{F/F}$ and LH2$^{F/F}$ OC-Cre mice, respectively. **(C)** LH3 levels are calculated by the IHC scoring system (n = 3). The LH3 IHC scores for the cells of the cancellous bone ranged from 64.6 to 78.1 (median, 72.6) and 56.7 to 76.4 (median, 69.4) in LH2$^{F/F}$ and LH2$^{F/F}$ OC-Cre mice, respectively. The LH3 IHC scores for the cells of the cortical bone ranged from 40.8 to 46.3 (median, 44.7) and 39.3 to 50.5 (median, 46.2) in LH2$^{F/F}$ and LH2$^{F/F}$ OC-Cre mice, respectively. **(D)** Representative IHC images for Col1 in cancellous and cortical regions of femurs from LH2$^{F/F}$ and LH2$^{F/F}$ OC-Cre mice. Col1 expression levels are not significantly different between LH2$^{F/F}$ and LH2$^{F/F}$ OC-Cre femurs. Original magnification, ×40 and × 200; Scale bars, 300 μm and 50 μm. Col1 levels are calculated by the IHC scoring system (n = 3). The Col1 IHC scores for the cells of the cancellous bone ranged from 64.7 to 84.0 (median, 73.6) and 62.4 to 77.5 (median, 67.4) in LH2$^{F/F}$ and LH2$^{F/F}$ OC-Cre mice, respectively. The Col1 IHC scores for the cells of the cortical bone ranged from 40.5 to 63.0 (median, 54.4) and 45.2 to 66.1 (median, 51.8) in LH2$^{F/F}$ and LH2$^{F/F}$ OC-Cre mice, respectively. **(E)** Volcano plots of significantly differentially expressed genes with $P < 0.05$ and more than a two-fold change or less than a 0.5-fold change in 75 upregulated and 250 downregulated proteins. The X-axis represents the (log2) fold-change (FC) and the Y-axis represents the − log10 of the *P*-value. **(F)** LH2 expression levels in LH2$^{F/F}$ OC-Cre femurs are significantly lower than in LH2$^{F/F}$ femurs. LH1, LH3, and Col1 expression levels are not significantly different between LH2$^{F/F}$ and LH2$^{F/F}$ OC-Cre femurs. *$P <$ 0.05; NS, Not significant.

2.8. Statistical analysis

The Welch's *t*-test were used to analyze statistical differences, and P-values below 0.05 were considered statistically significant. The data are expressed as the mean ± the standard deviation (SD).

3. Results

3.1. Generation of LH2$^{F/F}$ OC-Cre mice

The bsLH2-cKO was generated using the OC-Cre/loxP system. We performed PCR analysis of genomic DNA extracted from tails of six types of mice (LH2$^{+/+}$, LH2$^{+/+}$ OC-Cre, LH2$^{F/+}$, LH2$^{F/+}$ OC-Cre, LH2$^{F/F}$, and LH2$^{F/F}$ OC-Cre), using previously reported primer sets [25]. Since LH2 floxed (LH2^{F}) allele includes two loxP and a FRT sites, PCR product sizes of LH2^{F} and LH2^{+} alleles were 1028 bp and 926 bp, respectively, as shown in Fig. 1A (upper panel). We also used OC-Cre primers to confirm the bone-specific expression of Cre recombinase (Fig. 1A; lower panel).

Histological images of cancellous and cortical bones of femurs (LH2$^{F/F}$ and LH2$^{F/F}$ OC-Cre) are shown in Fig. 1B. Based on the H&E staining, there were no obvious differences in both regions between LH2$^{F/F}$ and LH2$^{F/F}$ OC-Cre mice. The LH2 protein levels in these regions of femurs were then assessed by IHC (Fig. 2A). The levels of immunoreactivities for LH2 in LH2$^{F/F}$ OC-Cre mice were significantly lower in both cancellous and cortical regions than those in LH2$^{F/F}$ mice (Fig. 2A; $P < 0.05$). In addition to the bone-associated cells, the hypertrophic chondrocytes in the growth plate also showed positive immunoreactivity for LH2 in LH2$^{F/F}$ mice but the reactivities were significantly lower in LH2$^{F/F}$ OC-Cre mice (yellow arrows). In the cortical bone, weak immunoreactivities were seen in osteocytes in LH2$^{F/F}$ mice (red arrows) but almost absent in LH2$^{F/F}$ OC-Cre mice. The LH2 IHC scores for the cells of cancellous bone areas ranged from 72.3 to 88.8 (median, 76.2) and 20.6 to 30.6 (median, 25.6) in LH2$^{F/F}$ and LH2$^{F/F}$ OC-Cre mice, respectively ($P < 0.001$), and those in the cortical bone ranged from 49.8 to 60.9 (median, 57.3) and 18.0 to 23.2 (median, 20.0) in LH2$^{F/F}$ and LH2$^{F/F}$ OC-Cre mice, respectively ($P < 0.05$).

3.2. Immunohistological evaluations of relevant proteins in femurs in LH2$^{F/F}$ OC-Cre mice

Protein levels of other LH isoforms, i.e. LH1 and LH3, in the cancellous and cortical bone areas of LH2$^{F/F}$ and LH2$^{F/F}$ OC-Cre femurs were assessed by IHC. Both LH1 and LH3 levels in both regions were not significantly different between LH2$^{F/F}$ and LH2$^{F/F}$ OC-Cre femurs (Fig. 2B and C). Col1 levels in these regions were also comparable between LH2$^{F/F}$ and LH2$^{F/F}$ OC-Cre femurs (Fig. 2D).

When subjected to PSR staining and observed under the polarized light, LH2$^{F/F}$ cancellous bones showed a certain directionality of thick fibers with green, orange and red colors indicating thick, tightly packed and organized collagen fibers in this group. However, LH2$^{F/F}$ OC-Cre cancellous bones showed a patchy appearance with a poor directionality with green to orange colors indicating that the collagen fibers are immature and are not packed in an orderly fashion (Fig. 3A). For the cortical bones, LH2$^{F/F}$ also showed a well-organized, lamellar structure with yellow to red colors while LH2$^{F/F}$ OC-Cre a poorly organized, non-lamellar structure with green to orange colors (Fig. 3A).

Quantitative image analysis under polarized light demonstrated that the staining intensities of the red fibers in LH2$^{F/F}$ OC-Cre mice were significantly lower than those of LH2$^{F/F}$ mice and the green significantly higher than those of LH2$^{F/F}$ mice (Fig. 3A).

3.3. Proteomic analysis of femurs in LH2$^{F/F}$ OC-Cre mice

We performed DIA proteomics analysis to assess the protein expression patterns in the femurs of LH2$^{F/F}$ OC-Cre mice as compared to those of LH2$^{F/F}$. Volcano plots revealed that 75 and 250 proteins were significantly up and downregulated more than two-fold, respectively, in LH2$^{F/F}$ OC-Cre femurs when compared to LH2$^{F/F}$ femurs (Fig. 2E). Consistent with the IHC data, LH2 expression was markedly decreased in LH2$^{F/F}$ OC-Cre mice (Fig. 2E and F; $P < 0.05$). LH1, LH3, and Col1 levels were not significantly different between LH2$^{F/F}$ OC-Cre and LH2$^{F/F}$ mice (Fig. 2E and F; $P > 0.05$).

3.4. Characterization of collagen fibrils and mCT analysis

Typical cross-sectional views of the collagen fibrils in the femurs from LH2$^{F/F}$ and LH2$^{F/F}$ OC-Cre mice are shown in Fig. 3B. The fibrils in the LH2$^{F/F}$ mice were generally circular in shape and relatively uniform while those in LH2$^{F/F}$ OC-Cre mice were irregular and frequently fused. The distribution range of fibril diameters in the LH2$^{F/F}$ bones was ~10–70 nm with a mean value of 38.09 nm. The LH2$^{F/F}$ OC-Cre mice showed wider diameters with a broad distribution range, i.e. 20–100 nm with a mean value of 51.02 nm. The difference in the diameter between the two groups was significant (Fig. 3B; $P < 0.001$).

We next evaluated bone mineral density (BMD) and bone volume (BV) using 10 μCT slices from each of the 4 mice (n = 4). While there were no significant differences in cortical and cancellous BV between LH2$^{F/F}$ and LH2$^{F/F}$ OC-Cre femurs, the BMDs of both cortical and

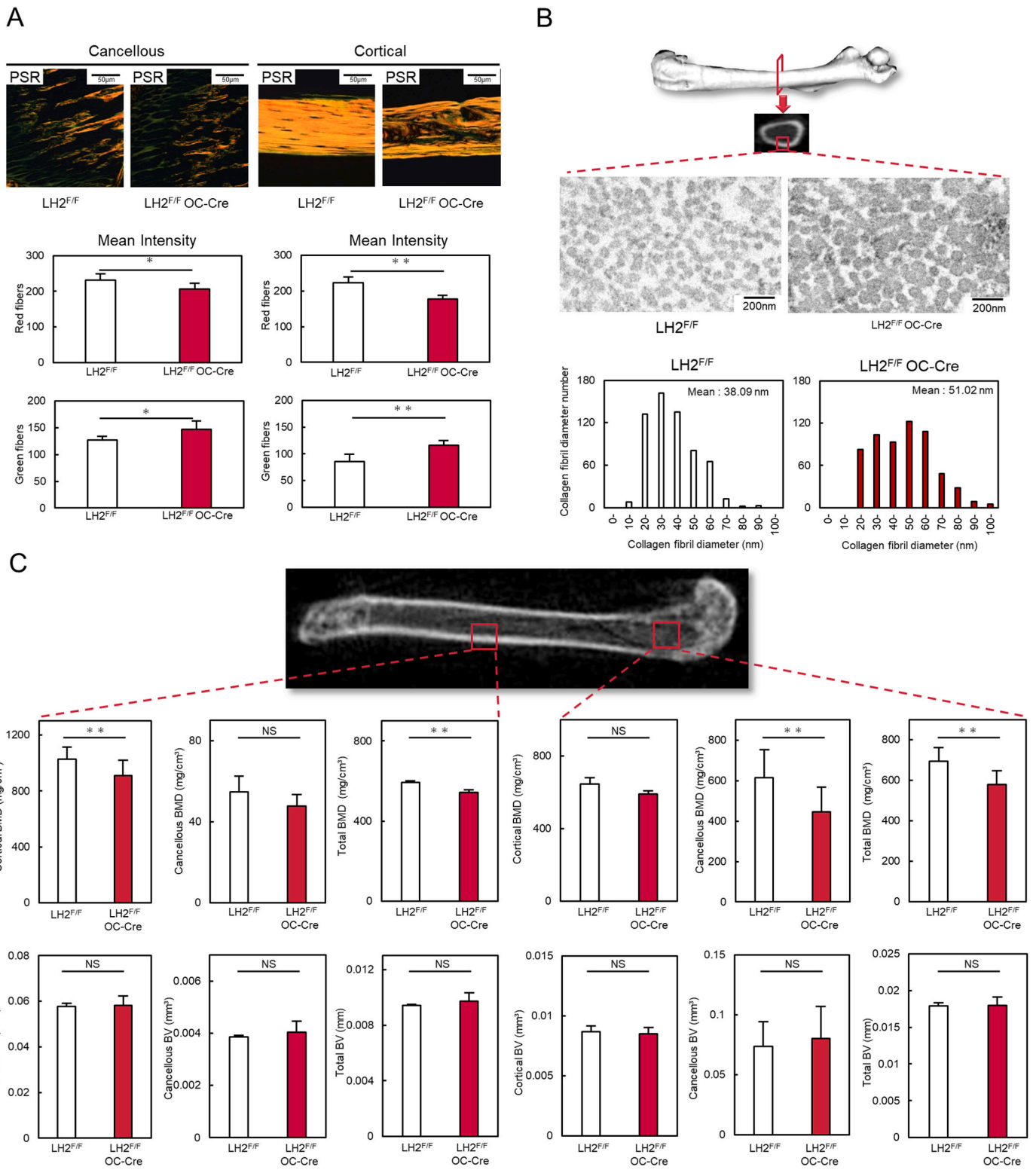

(caption on next page)

Fig. 3. Histological evaluation, TEM and μCT analyses of femurs in LH2$^{F/F}$ OC-Cre mice (PSR). (A) Representative PSR images of cancellous and cortical regions of femurs from LH2$^{F/F}$ and LH2$^{F/F}$ OC-Cre mice. PSR staining quantification of the mean intensity of red and green fibers in the cancellous and cortical regions. The collagen fibers in the LH2$^{F/F}$ OC-Cre femurs show a green and, in some areas, orange/red color, whereas those of LH2$^{F/F}$ femurs show a relatively uniform orange color. The mean intensity of red fibers in the cancellous and cortical regions of femurs from LH2$^{F/F}$ OC-Cre is significantly lower than those of LH2$^{F/F}$ femurs. The mean intensity of green fibers in the cancellous and cortical regions of femurs from LH2$^{F/F}$ OC-Cre is significantly higher than those of LH2$^{F/F}$ femurs. **(B)** Cross-section of femoral collagen fibrils in LH2$^{F/F}$ and LH2$^{F/F}$ OC-Cre mice under TEM. A total of 600 fibrils were measured for each sample and plotted. Collagen fibrils of femurs in LH2$^{F/F}$ OC-Cre mice show an irregular distribution of fibril diameters, and the average diameter of collagen fibrils in LH2$^{F/F}$ OC-Cre mice is significantly larger than that in LH2$^{F/F}$ mice. 600 fibrils in each group were measured from a single experiment and plotted. **(C)** Representative μCT images of the coronal section of femurs (n = 4). Parameters for the CT scans were set as follows: tube voltage, 50 kVp; tube current, 145 μA; integration time, 3.6 ms; axial field of view, 60 mm, with an isotropic voxel size of 60 × 30 μm, according to the manufacturer's instructions. Regions of interest (ROI) were defined as areas of cancellous bones below the proximal growth plate (proximal portion) and the cortical bones in the central portion of the femur. In the cortical area, cortical BMD is significantly lower than in the femurs of LH2$^{F/F}$. In the cancellous area of LH2$^{F/F}$ OC-Cre femurs, cancellous BMD and total BMD are significantly lower than in the femurs of LH2$^{F/F}$ mice. Cortical BV, cancellous BV, and total BV are not significantly different between LH2$^{F/F}$ and LH2$^{F/F}$ OC-Cre femurs. *$P < 0.05$; **$P < 0.01$; and ***$P < 0.001$; NS, Not significant. (For interpretation of the references to color in this figure legend, the reader is referred to the Web version of this article.)

cancellous regions in LH2$^{F/F}$ OC-Cre femurs were significantly lower than in LH2$^{F/F}$ femurs (Fig. 3C; $P < 0.01$).

3.5. Bone mechanical properties of femurs

We then assessed the biomechanical properties of LH2$^{F/F}$ and LH2$^{F/F}$ OC-Cre femurs using the three-point bending tests (Fig. 4A). The results revealed that the elapsed time of breaking point, maximum load, breaking load, breaking times, breaking placement, breaking energy, and stiffness in LH2$^{F/F}$ OC-Cre femurs were all significantly lower than those in LH2$^{F/F}$ femurs (Fig. 4B and C). These results demonstrated that the load-bearing capacities in LH2$^{F/F}$ OC-Cre femurs were markedly lower, i.e. more fragile, than those of LH2$^{F/F}$, suggesting that LH2-catalyzed collagen post-translational modifications are critical for bone mechanical strength.

3.6. Collagen cross-link analysis of femurs in LH2$^{F/F}$ OC-Cre mice

The amino acid analysis revealed that the Hyl content in collagen, calculated as Hyl/HypX300, was significantly decreased in LH2$^{F/F}$ OC-Cre femurs compared to that of LH2$^{F/F}$ (Fig. 5A; $P < 0.001$). Using the mass spectrometric analysis, we evaluated the extent of Lys hydroxylation in the telopeptides of Col1. The results demonstrated that, in LH2$^{F/F}$ OC-Cre collagen, Lys residues in the α1 chain telepeptides (α1 Lys-9^{N} and α1 Lys-16^{C}) were both significantly ($P < 0.05$) under-hydroxylated compared to those of LH2$^{F/F}$ by ~80–90 % (Fig. 5B). There was a trend of lower Hyl at α2 Lys-5^{N} in LH2$^{F/F}$ OC-Cre Col1 that of LH2$^{F/F}$ but did not reach the significant level (Fig. 5B). In all bone samples, reducible cross-links, DHLNL, HLNL and HHMD, and non-reducible cross-links Pyr and d-Pyr were identified and quantified. The results demonstrated that the Hyl^{ald}-derived cross-links, thus, LH2-mediated cross-links, Pyr, and DHLNL were significantly ($P < 0.01$) decreased in LH2$^{F/F}$ OC-Cre femurs compared to LH2$^{F/F}$ femurs (Fig. 5C). Another LH2-mediated cross-link, d-Pyr, trended lower in LH2$^{F/F}$ OC-Cre femurs, but the difference did not reach the significant level (Fig. 5C; $P > 0.05$). HLNL was markedly increased in LH2$^{F/F}$ OC-Cre mice when compared to LH2$^{F/F}$ mice (Fig. 5C). Even though this cross-link can be derived from Lys^{ald} × Hyl or Hyl^{ald} × Lys, given that telopeptidyl Lys hydroxylation in LH2$^{F/F}$ OC-Cre collagen was markedly decreased, the increase of HLNL in LH2$^{F/F}$ OC-Cre collagen is most likely the result of the increase of (Lys^{ald} × Hyl) not (Hyl^{ald} × Lys). The ratio of DHLNL to HLNL was significantly decreased in LH2$^{F/F}$ OC-Cre femur collagen (Fig. 5C). The HHMD cross-link, a non-LH2-mediated cross-link, tended to be lower in LH2$^{F/F}$ OC-Cre femur collagen though the difference was not significant (Fig. 5C). The ratio of the Hyl^{ald}- (DHLNL, Pyr, and d-Pyr) to Lys^{ald}-derived (HHMD) cross-links, i.e., LH2-mediated to -non-mediated cross-links, were significantly ($P < 0.01$) lower in LH2$^{F/F}$ OC-Cre femurs than in LH2$^{F/F}$ femurs (Fig. 5C). The total number of aldehydes involved in cross-linking was significantly decreased in LH2$^{F/F}$ OC-Cre femurs compared to LH2$^{F/F}$ femurs ($P < 0.05$) (Fig. 5C).

4. Discussion

The function of LH2 as telopeptidyl LH has been reported by several groups employing correlational as well as gain-/loss-of-function studies [17,27–29]. These early studies, however, primarily depended on the collagen cross-link profile to characterize the state of telopeptidyl Lys hydroxylation. Also, in these studies, no complete LH2 gene (*Procollagen-Lysine, 2-Oxoglutarate 5-Dioxygenase 2; Plod2*) knockout cells or animal models were established. Our attempt to generate the *Plod2* knockout mice to study the LH2 function at the tissue and animal levels was unsuccessful due to its early embryonic lethality [24]. Recently, with the progress of proteomics and gene editing technology, we have generated *Plod2* knockout osteoblastic cells and characterized molecular phenotypes of Col1 and its functional outcomes [20]. Gistelinck and co-workers have generated a *Plod2* non-sense zebrafish model and showed its adverse effects on musculoskeletal development [30]. The same group also analyzed bone Col1 in a patient with type II BS caused by *PLOD2* mutations and reported the lack of telopeptidyl Lys hydroxylation in the sample. We have also reported bone phenotypes in LH2 heterozygous mice that expressed low levels of LH2 in this mouse model. These *in vivo* studies have provided valuable insights into the function of LH2 in bone development. However, a question remains: Do the bone phenotypes observed in the LH2 mutant/deficient animals occur specifically in bone, if so, what would be the mechanisms, or are these phenotypes a result of LH2 deficiency in the whole animal? To partially address this question, we generated bone-specific LH2 conditional knockout mice.

In the present study, we reported the generation of bsLH2-cKO mice using an OC-Cre/loxP system and demonstrated that deficiency of LH2 in OC-expressing mature osteoblasts significantly affected the molecular phenotypes of bone Col1, i.e. telopeptidyl Lys hydroxylation, cross-linking, collagen fibrillogenesis, and bone quality as evaluated by BMD and mechanical properties.

The Cre/loxP system is one of the most widely used techniques to generate tissue-specific gene knockout mice. Several types of Cre mice, such as OC-Cre, Osx-Cre, and Col1-Cre, have been used to generate bone-specific conditional KO mice. Among them, we had adopted the OC-Cre system because OC-Cre transgene becomes active beginning at E17 when bone formation begins [31], targets the mature osteoblast lineage including osteocytes, and the activity is not detected in non-skeletal tissues [31]. We first confirmed that the expression of LH2 was significantly suppressed in bone without affecting other LH members, LH1 and 3, or Col1 (Fig. 2). This was also confirmed by DIA proteomics analysis showing a marked suppression of LH2 (10-fold downregulation in bsLH2-cKO bone) but no differences in LH1, 3 and Col1 (Fig. 2). Small amounts of LH2 seen in IHC as well as DIA analyses of bone indicate that LH2 is also expressed in cells such as preosteoblasts other than mature osteoblasts, and osteocytes and hypertrophic chondrocytes where osteocalcin is significantly expressed [32]. Incomplete recombination efficiency and a potential off-target recombination [33] could also be contributing factors. These need to be addressed in future studies.

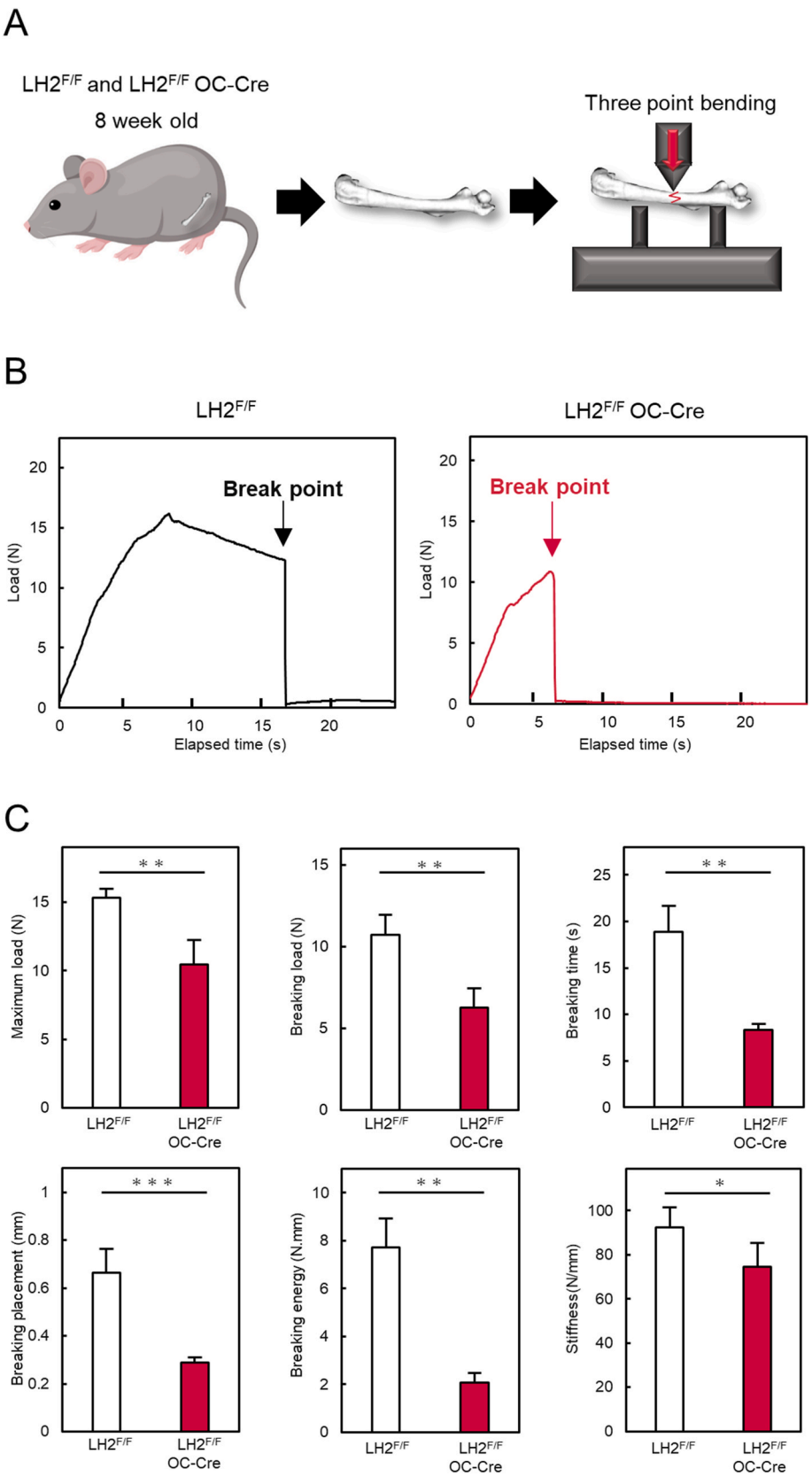

Fig. 4. Bone mechanical strength of femurs in LH2$^{F/F}$ OC-Cre mice. Mechanical properties of LH2$^{F/F}$ and LH2$^{F/F\ OC\text{-}Cre}$ femurs (n = 4). **(A)** Illustration of the three-point bending test in LH2$^{F/F}$ and LH2$^{F/F}$ OC-Cre mice. **(B, C)** Maximum load, breaking load, breaking times, breaking placement, elapsed time of breaking point, breaking energy, and stiffness in LH2$^{F/F}$ OC-Cre femurs are significantly lower than in LH2$^{F/F}$ femurs. *$P < 0.05$; **$P < 0.01$; and ***$P < 0.001$.

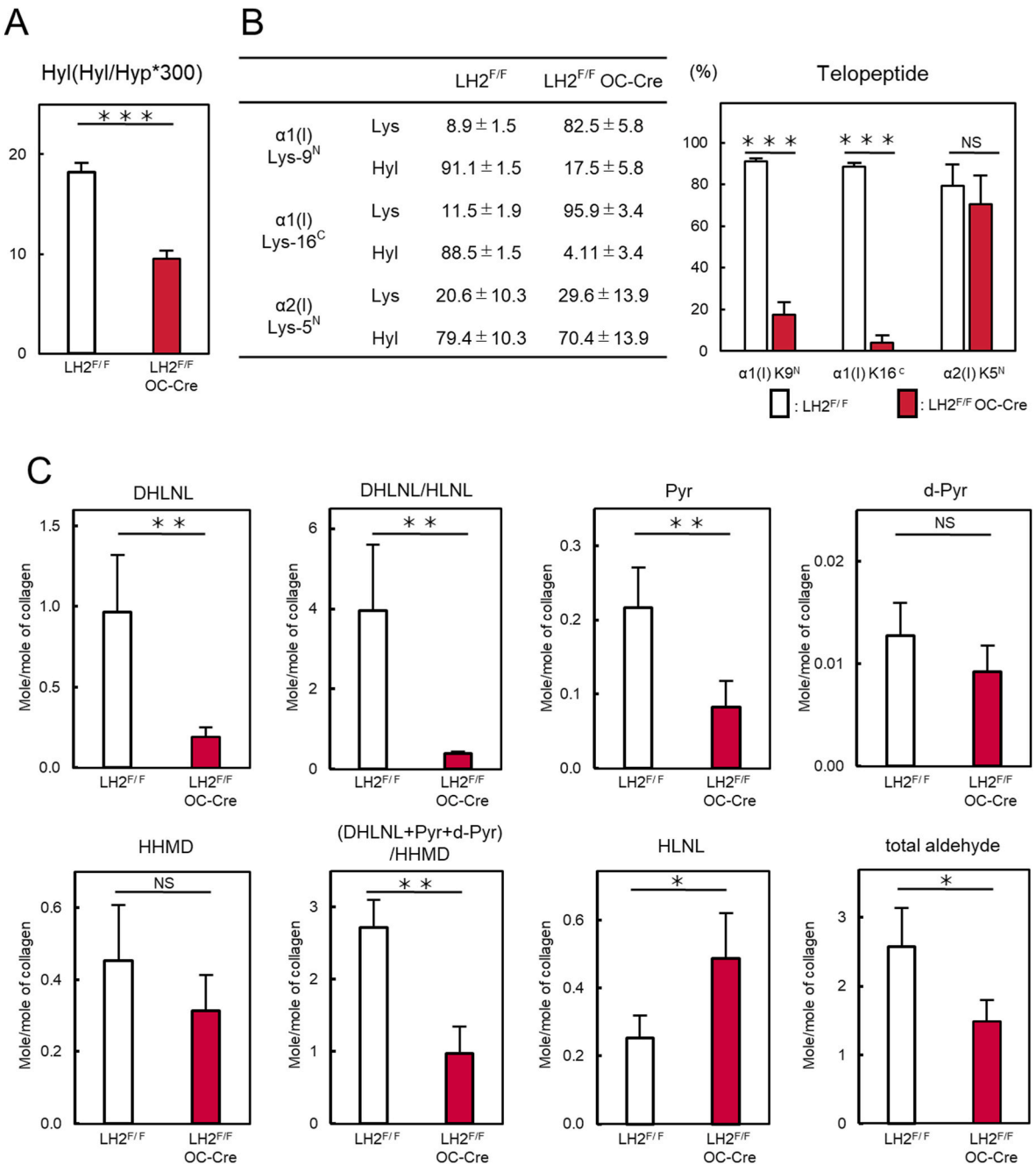

Fig. 5. Collagen cross-link and lysine hydroxylation analyses of femurs in LH2$^{F/F}$ OC-Cre mice. (A) Amino acid analysis quantified as moles/mol of collagen (n = 4). Hyl (Hyl/HypX300) are significantly lower in LH2$^{F/F}$ OC-Cre femurs than LH2$^{F/F}$ femurs. **(B)** Lysine hydroxylation is expressed as a percentage calculated by hydroxylysine/(lysine + hydroxylysine) × 100. between LH2$^{F/F}$ (n = 4) and LH2$^{F/F}$ OC-Cre (n = 4), respectively. **(C)** Cross-links were quantified as moles/mol of collagen (n = 4). DHLNL, DHLNL/HLNL, Pyr, total aldehydes, and the ratio of the Hyl^{ald} to Lys^{ald}-derived cross-links are significantly lower in LH2$^{F/F}$ OC-Cre than in LH2$^{F/F}$ mice, whereas those of HHMD are not different between the mice. DHLNL, dihydroxylysinonorlucine; d-Pyr, deoxypyridinoline; Pyr, pyridinoline; HHMD, histidinohydroxymerodesmosine; HLNL, hydroxylysinonorleucine; total aldehyde, number of aldehydes involved in the cross-links calculated as DHLNL + HLNL +2 × Pyr + 2 × d-Pyr + 2 × HHMD; (DHLNL + Pyr + d-Pyr)/HHMD indicates the ratio of the hydroxylysine aldehyde (Hyl^{ald})- to lysine aldehyde (Lys^{ald})-derived cross-links. *$P < 0.05$; **$P < 0.01$; and ***$P < 0.001$; NS, Not significant.

Interestingly, osteocalcin-expressing tissues such as cartilage (Fig. 1B) and ligament [34] appear unaffected at least at the light microscopic level indicating that LH2 deficiency mainly impair bone tissues. Expression levels of major cartilage components such as type II collagen (Col2) and aggrecan were not significantly changed in LH2$^{F/F}$ OC-Cre mice compared with LH2$^{F/F}$ (Appendix Fig. 1). The tissue-specific effect of LH2 deficiency needs to be addressed in future studies. As for the collagen phenotypes in bsLH2-cKO bones, at the light microscopic level, collagen fibers in both cancellous and cortical bones appear to be immature and less organized compared to those of controls (Fig. 3A). At the ultrastructural level, collagen fibrils in bsLH2-cKO bones were frequently fused and showed a broad distribution of fibril diameters (Fig. 3B). Since fibrillar Col1 functions as a 3-dimensional template for mineralization [35], such structural abnormalities likely cause defective mineralization of bone leading to lower BMD and inferior mechanical properties (Figs. 3C and 4).

As expected, an extent of Lys hydroxylation in Col1 telopeptides in bsLH2-cKO bone was significantly lower than that of controls. This is

consistent with the data of LH2 heterozygous mouse bones, LH2 mutant zebrafish bones [30], bone from a BS patient [36] and LH2-KO osteoblastic cells [20]. Interestingly, though showing a trend, the a2(I) N-telopeptide Lys hydroxylation was relatively unaffected when compared to the N- and C-telopeptides of a1(I) chain. The similar finding, i.e. less affected Lys hydroxylation in the a2(I) N-telopeptide, was also reported in LH2 heterozygous bone collagen and that secreted by LH2-KO osteoblastic cells [20]. This could be due to its sequence, -Asp-Lys-Gly-, that also occur in the helical domains, i.e. two in an a1 and one in an a2 chains in mouse Col1 (Uniprot numbers P11807 and Q01149), thus, it can be hydroxylated by the helical lysyl hydroxylase, LH1. These changes in the telopeptidyl Lys hydroxylation led to a significant reduction of Hyl^{ald}-derived stable cross-links in the LH2cKO bone collagen that result in increased solubility and enzymatic degradability of collagen [20]. Furthermore, we found a significant reduction of total aldehydes involved in cross-linking in bsLH2-cKO bone. These changes in cross-linking may partially explain the immature and less organized collagen matrix seen in the bsLH2-cKO bone, thus, affecting their mechanical properties.

In conclusion, we generated the bsLH2-cKO mice and demonstrated the defects in type I collagen and inferior mechanical properties of bone in these mice. These findings indicate that bone defects caused by PLOD2 mutations seen in BS may occur in an osteoblast-specific manner. This mouse model may provide further insights into the role of LH2 catalyzed type I collagen modifications in bone formation and pathologies.

CRediT authorship contribution statement

Kenta Tsuneizumi: Writing – original draft, Formal analysis, Data curation. **Atsushi Kasamatsu:** Writing – review & editing, Writing – original draft. **Tomoaki Saito:** Investigation, Formal analysis. **Reo Fukushima:** Formal analysis, Data curation. **Yuki Taga:** Formal analysis, Data curation. **Kazunori Mizuno:** Formal analysis, Data curation. **Masataka Sunohara:** Investigation, Formal analysis. **Katsuhiro Uzawa:** Writing – review & editing, Writing – original draft. **Mitsuo Yamauchi:** Writing – review & editing, Writing – original draft.

Declaration of competing interest

The authors declare that they have no known competing financial interests or personal relationships that could have appeared to influence the work reported in this paper.

Data availability

Data will be made available on request.

Acknowledgments

This work was supported by JSPS KAKENHI, Fostering Joint International Research (B), Grant Number JP21KK0159.

Appendix A. Supplementary data

Supplementary data to this article can be found online at https://doi.org/10.1016/j.bbrep.2024.101790.

References

[1] S. Ricard-Blum, The collagen family, Cold Spring Harbor Perspect. Biol. 3 (2011) 1–19, https://doi.org/10.1101/cshperspect.a004978.
[2] M. Yamauchi, M. Sricholpech, Lysine post-translational modifications of collagen, Essays Biochem. 52 (2012) 113–133, https://doi.org/10.1042/BSE0520113.
[3] V.T. Ha, M.K. Marshall, L.J. Elsas, S.R. Pinnell, H.N. Yeowell, A patient with Ehlers-Danlos syndrome type VI is a compound heterozygote for mutations in the lysyl hydroxylase gene, J. Clin. Invest. 93 (1994) 1716–1721, https://doi.org/10.1172/JCI117155.
[4] H.N. Yeowell, L.C. Walker, Mutations in the lysyl hydroxylase 1 gene that result in enzyme deficiency and the clinical phenotype of Ehlers-Danlos syndrome type VI, Mol. Genet. Metabol. 71 (2000) 212–224, https://doi.org/10.1006/mgme.2000.3076.
[5] Y. Ishikawa, J.A. Vranka, S.P. Boudko, E. Pokidysheva, K. Mizuno, K. Zientek, D. R. Keene, A.M. Rashmir-Raven, K. Nagata, N.J. Winand, H.P. Bächinger, Mutation in cyclophilin B that causes hyperelastosis cutis in american quarter horse does not affect peptidylprolyl cis-trans isomerase activity but shows altered cyclophilin b-protein interactions and affects collagen folding, J. Biol. Chem. 287 (2012), https://doi.org/10.1074/jbc.M111.333336.
[6] M. Shiiba, S.B. Arnaud, H. Tanzawa, E. Kitamura, M. Yamauchi, Regional alterations of type I collagen in rat tibia induced by skeletal unloading, J. Bone Miner. Res. 17 (2002) 1639–1645, https://doi.org/10.1359/jbmr.2002.17.9.1639.
[7] A.J. Van der Slot, A.M. Zuurmond, A.F.J. Bardoel, C. Wijmenga, H.E.H. Pruijs, D. O. Sillence, J. Brinckmann, D.J. Abraham, C.M. Black, N. Verzijl, J. DeGroot, R. Hanemaaijer, J.M. TeKoppele, T.W.J. Huizinga, R.A. Bank, Identification of PLOD2 as telopeptide lysyl hydroxylase, an important enzyme in fibrosis, J. Biol. Chem. 278 (2003) 40967–40972, https://doi.org/10.1074/jbc.M307380200.
[8] A.J. van der Slot, A.-M. Zuurmond, A.J. van den Bogaerdt, M.M.W. Ulrich, E. Middelkoop, W. Boers, H. Karel Ronday, J. DeGroot, T.W.J. Huizinga, R.A. Bank, Increased formation of pyridinoline cross-links due to higher telopeptide lysyl hydroxylase levels is a general fibrotic phenomenon, Matrix Biol. 23 (2004) 251–257, https://doi.org/10.1016/j.matbio.2004.06.001.
[9] A.J. Van Der Slot-Verhoeven, E.A. Van Dura, J. Attema, B. Blauw, J. DeGroot, T.W. J. Huizinga, A.M. Zuurmond, R.A. Bank, The type of collagen cross-link determines the reversibility of experimental skin fibrosis, Biochim. Biophys. Acta, Mol. Basis Dis. 1740 (2005), https://doi.org/10.1016/j.bbadis.2005.02.007.
[10] K. Uzawa, M.K. Marshall, E.P. Katz, H. Tanzawa, H.N. Yeowell, M. Yamauchi, Altered Posttranslational Modifications of Collagen in Keloid, 1998.
[11] A.M. Salo, H. Cox, P. Farndon, C. Moss, H. Grindulis, M. Risteli, S.P. Robins, R. Myllylä, A connective tissue disorder caused by mutations of the lysyl hydroxylase 3 gene, Am. J. Hum. Genet. 83 (2008), https://doi.org/10.1016/j.ajhg.2008.09.004.
[12] S.A. Watt, J.H.S. Dayal, S. Wright, M. Riddle, C. Pourreyron, J.R. McMillan, R. M. Kimble, M. Prisco, U. Gartner, E. Warbrick, W.H. Irwin McLean, I.M. Leigh, J. A. McGrath, J.C. Salas-Alanis, J. Tolar, A.P. South, Lysyl hydroxylase 3 localizes to epidermal basement membrane and is reduced in patients with recessive dystrophic epidermolysis bullosa, PLoS One 10 (2015), https://doi.org/10.1371/journal.pone.0137639.
[13] W.A. Cabral, I. Perdivara, M.A. Weis, M. Terajima, A.R. Blissett, W. Chang, J. E. Perosky, E.N. Makareeva, E.L. Mertz, S. Leikin, K.B. Tomer, K.M. Kozloff, D. R. Eyre, M. Yamauchi, J.C. Marini, Abnormal type I collagen post-translational modification and crosslinking in a cyclophilin B KO mouse model of recessive osteogenesis imperfecta, PLoS Genet. 10 (2014), https://doi.org/10.1371/journal.pgen.1004465.
[14] Y. Chen, H. Guo, M. Terajima, P. Banerjee, X. Liu, J. Yu, A.A. Momin, H. Katayama, S.M. Hanash, A.R. Burns, G.B. Fields, M. Yamauchi, J.M. Kurie, Lysyl hydroxylase 2 is secreted by tumor cells and can modify collagen in the extracellular space, J. Biol. Chem. 291 (2016) 25799–25808, https://doi.org/10.1074/jbc.M116.759803.
[15] M. Terajima, Y. Taga, W.A. Cabral, M. Nagasawa, N. Sumida, S. Hattori, J. C. Marini, M. Yamauchi, Cyclophilin B deficiency causes abnormal dentin collagen matrix, J. Proteome Res. 16 (2017) 2914–2923, https://doi.org/10.1021/acs.jproteome.7b00190.
[16] M. Terajima, Y. Taga, W.A. Cabral, Y. Liu, M. Nagasawa, N. Sumida, Y. Kayashima, P. Chandrasekaran, L. Han, N. Maeda, I. Perdivara, S. Hattori, J.C. Marini, M. Yamauchi, Cyclophilin B control of lysine post-translational modifications of skin type I collagen, PLoS Genet. 15 (2019), https://doi.org/10.1371/journal.pgen.1008196.
[17] K. Uzawa, W.J. Grzesik, T. Nishiura, S.A. Kuznetsov, P. Gehron Robey, D. A. Brenner, M. Yamauchi, Differential expression of human lysyl hydroxylase genes, lysine hydroxylation, and cross-linking of type I collagen during osteoblastic differentiation in vitro, J. Bone Miner. Res. 14 (1999) 1272–1280, https://doi.org/10.1359/jbmr.1999.14.8.1272.
[18] S. Pornprasertsuk, W.R. Duarte, Y. Mochida, M. Yamauchi, Lysyl hydroxylase-2b directs collagen cross-linking pathways in MC3T3-E1 cells, J. Bone Miner. Res. 19 (2004) 1349–1355, https://doi.org/10.1359/JBMR.040323.
[19] B. Piersma, R.A. Bank, Collagen cross-linking mediated by lysyl hydroxylase 2: an enzymatic battlefield to combat fibrosis, Essays Biochem. 63 (2019) 377–387, https://doi.org/10.1042/EBC20180051.
[20] M. Terajima, Y. Taga, T. Nakamura, H.F. Guo, Y. Kayashima, N. Maeda-Smithies, K. Parag-Sharma, J.S. Kim, A.L. Amelio, K. Mizuno, J.M. Kurie, M. Yamauchi, Lysyl hydroxylase 2 mediated collagen post-translational modifications and functional outcomes, Sci. Rep. 12 (2022), https://doi.org/10.1038/s41598-022-18165-0.
[21] R.A.F. Gjaltema, M.M. Van Der Stoel, M. Boersema, R.A. Bank, Disentangling mechanisms involved in collagen pyridinoline cross-linking: the immunophilin FKBP65 is critical for dimerization of lysyl hydroxylase 2, Proc. Natl. Acad. Sci. U. S. A. 113 (2016) 7142–7147, https://doi.org/10.1073/pnas.1600074113.
[22] Y. Chen, M. Terajima, P. Banerjee, H. Guo, X. Liu, J. Yu, M. Yamauchi, J.M. Kurie, FKBP65-dependent peptidyl-prolyl isomerase activity potentiates the lysyl hydroxylase 2-driven collagen cross-link switch, Sci. Rep. 7 (2017), https://doi.org/10.1038/srep46021.
[23] G.A. Otaify, M.S. Abdel-Hamid, N.F. Hassib, R.M. Elhossini, S.F. Abdel-Ghafar, M. S. Aglan, Bruck syndrome in 13 new patients: identification of five novel FKBP10

and PLOD2 variants and further expansion of the phenotypic spectrum, Am. J. Med. Genet. 188 (2022) 1815–1825, https://doi.org/10.1002/ajmg.a.62718.
[24] A. Kasamatsu, K. Uzawa, F. Hayashi, A. Kita, Y. Okubo, T. Saito, Y. Kimura, I. Miyamoto, N. Oka, M. Shiiba, C. Ito, K. Toshimori, T. Miki, M. Yamauchi, H. Tanzawa, Deficiency of lysyl hydroxylase 2 in mice causes systemic endoplasmic reticulum stress leading to early embryonic lethality, Biochem. Biophys. Res. Commun. 512 (2019) 486–491, https://doi.org/10.1016/j.bbrc.2019.03.091.
[25] R. Nozaki, A. Kasamatsu, J. Moss, K. Uzawa, Lysyl hydroxylase 2 deficiency promotes filopodia formation and fibroblast migration, Biochem. Biophys. Res. Commun. 587 (2022) 146–152, https://doi.org/10.1016/j.bbrc.2021.11.100.
[26] J.P. Rose, C.A. Schurman, C.D. King, J. Bons, J.B. Burton, S.K. Patel, A. O'Broin, T. Alliston, B. Schilling, Deep coverage and quantification of the bone proteome provides enhanced opportunities for new discoveries in skeletal biology and disease, bioRxiv 2022 (2023) 517228, https://doi.org/10.1101/2022.11.20.517228, 11.20.
[27] D.K. Mercer, P.F. Nicol, C. Kimbembe, S.P. Robins, Identification, expression, and tissue distribution of the three rat lysyl hydroxylase isoforms, Biochem. Biophys. Res. Commun. 307 (2003) 803–809, https://doi.org/10.1016/S0006-291X(03)01262-2.
[28] S. Pornprasertsuk, W.R. Duarte, Y. Mochida, M. Yamauchi, Lysyl hydroxylase-2b directs collagen cross-linking pathways in MC3T3-E1 cells, J. Bone Miner. Res. 19 (2004) 1349–1355, https://doi.org/10.1359/JBMR.040323.
[29] A.J. Van Der Slot-Verhoeven, E.A. Van Dura, J. Attema, B. Blauw, J. DeGroot, T.W. J. Huizinga, A.M. Zuurmond, R.A. Bank, The type of collagen cross-link determines the reversibility of experimental skin fibrosis, Biochim. Biophys. Acta, Mol. Basis Dis. 1740 (2005) 60–67, https://doi.org/10.1016/j.bbadis.2005.02.007.
[30] C. Gistelinck, P.E. Witten, A. Huysseune, S. Symoens, F. Malfait, D. Larionova, P. Simoens, M. Dierick, L. Van Hoorebeke, A. De Paepe, R.Y. Kwon, M.A. Weis, D. R. Eyre, A. Willaert, P.J. Coucke, Loss of type I collagen telopeptide lysyl hydroxylation causes musculoskeletal abnormalities in a zebrafish model of Bruck syndrome, J. Bone Miner. Res. 31 (2016) 1930–1942, https://doi.org/10.1002/jbmr.2977.
[31] J. McKenzie, C. Smith, K. Karuppaiah, J. Langberg, M.J. Silva, D.M. Ornitz, Osteocyte death and bone overgrowth in mice lacking fibroblast growth factor receptors 1 and 2 in mature osteoblasts and osteocytes, J. Bone Miner. Res. 34 (2019) 1660–1675, https://doi.org/10.1002/jbmr.3742.
[32] S. Kannan, J. Ghosh, S.K. Dhara, Osteogenic differentiation potential of porcine bone marrow mesenchymal stem cell subpopulations selected in different basal media, Biol. Open. 9 (2020), https://doi.org/10.1242/BIO.053280.
[33] S.L. Dallas, Y. Xie, L.A. Shiflett, Y. Ueki, Mouse Cre models for the study of bone diseases, Curr. Osteoporos. Rep. 16 (2018) 466–477, https://doi.org/10.1007/s11914-018-0455-7.
[34] M. Morishita, T. Yamamura, M.A. Bachchu, A. Shimazu, Y. Iwamoto, The effects of oestrogen on osteocalcin production by human periodontal ligament cells, Arch. Oral Biol. 43 (1998) 329–333, https://doi.org/10.1016/s0003-9969(97)00114-3.
[35] W.J. Landis, R. Jacquet, Association of calcium and phosphate ions with collagen in the mineralization of vertebrate tissues, Calcif. Tissue Int. 93 (2013) 329–337, https://doi.org/10.1007/s00223-013-9725-7.
[36] C. Gistelinck, M.A. Weis, J. Rai, U. Schwarze, D. Niyazov, K.M. Song, P.H. Byers, D. R. Eyre, Abnormal bone collagen cross-linking in osteogenesis imperfecta/bruck syndrome caused by compound heterozygous PLOD2 mutations, JBMR Plus 5 (2021), https://doi.org/10.1002/jbm4.10454.